

Effect Analysis of Spacer Stiffness and Interval on Galloping of Power Transmission Lines

Yun-Ji Oh*, Jeong-Hyun Sohn**,#

*Graduate School of Mechanical Design Engineering, PKNU, **Department of Mechanical Design Engineering, PKNU

스페이서 강성과 간격이 송전선 갤러핑에 미치는 영향분석

오윤지*, 손정현**,#

*부경대학교 일반대학원 기계설계공학과, **부경대학교 기계설계공학과

(Received 17 December 2018; received in revised form 29 December 2018; accepted 1 January 2019)

ABSTRACT

Due to icing and snow, power transmission lines have asymmetric cross sections, and their motion becomes unstable. At this time, the vibration caused by the wind is called galloping. If galloping is continuous, short circuits or ground faults may occur. It is possible to prevent galloping by installing spacers between transmission lines. In this study, the transmission line is modeled as a mass-spring-damper system by using RecurDyn. To analyze the dynamic behavior of the transmission line, the damping coefficient is derived from the free vibration test of the transmission line and Rayleigh damping theory. The drag and lift coefficient for modeling the wind load are calculated from the flow analysis by using ANSYS Fluent. Galloping simulations according to spacer stiffness and interval are carried out. It is found that when the stiffness is 100 N/m and the interval around the support is dense, the galloping phenomenon is reduced the most.

Key Words : Power Transmission Line(송전선), Galloping(갤러핑), Aerodynamic Coefficient(공기력계수), Spacer(스페이서)

1. Introduction

Transmission lines that pass through alpine areas and regions with heavy snowfall become aerodynamically unstable as their cross sections become asymmetric because of ice and snow accretion. If a strong wind blows over ice accretion

on transmission line, excessive vibration may occur because of the self-weight and tension of the transmission line, which is called galloping. When vibration occurs because of galloping, arcs occur between transmission line and short circuits or a ground fault is generated. Also, voltage sag occurs, thereby causing a fault current. The mixed contact short circuit of transmission line due to galloping has sometimes occurred in Korea. Moreover, the

Corresponding Author : jhsohn@pknu.ac.kr

Tel: 051-629-6166

Copyright © The Korean Society of Manufacturing Process Engineers. This is an Open-Access article distributed under the terms of the Creative Commons Attribution-Noncommercial 3.0 License (CC BY-NC 3.0 <http://creativecommons.org/licenses/by-nc/3.0>) which permits unrestricted non-commercial use, distribution, and reproduction in any medium, provided the original work is properly cited.



Fig. 1 Spring spacer

number of occurrences suddenly increased in the winter of 2012, with five accidents in two months. To prevent this type of accident, a variety of methods have been employed, such as an air flow spoiler that prevents a constant cross section according to a transmission line length and an anti-snow accretion ring that prevents ice accretion on transmission line. Among these methods, a phase spacer has been widely used, as shown in Figure 1, which prevents galloping by reducing the transmission line movements^[1-5].

The galloping phenomenon in transmission lines has been studied in the USA since 1990. Through wind tunnel experiments, Davison measured a change in the lift force with respect to an incident angle by using the asymmetrical form of the cross section of transmission lines^[6].

Den Hartog discovered that lift and drag forces change with variations in the incident angle and that transmission lines become unstable when an inclination of the lift is larger than the drag force^[7]. Kim performed galloping simulations about variable wind speed using RecurDyn, which is a multi-body commercial dynamics analysis program^[8]. Gwak conducted vibration measurement tests of bundled transmission lines on which spring spacers were installed using the image measurement method and verified the validity of the dynamic model of transmission lines^[9].

This study analyzed the effects of the stiffness of spring spacers located between bundled transmission line and installation spacing on galloping transmission line.

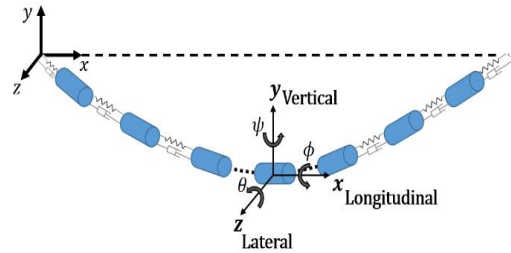


Fig. 2 System coordinate of transmission line

2. Modeling of transmission line

2.1 Dynamic modeling of transmission line

This study modeled transmission line using RecurDyn to analyze the galloping phenomenon dynamically. The coordinate for transmission line modeling is defined in Figure 2. The transmission line was modeled using a number of lumped masses, springs, and dampers, and a transmission line with 500 m span was modeled with 31 mass elements and 32 springs and dampers with consideration of the accuracy of the real model and the analysis time. Since the movement with respect to angles θ and ψ was relatively small compared to the sleet jump and galloping in Figure 2, a motion equation was not taken into consideration, and supporting points of the transmission line were assumed as fixed. Each of the lumped masses had four degrees of freedom (DOF) (x, y, z, ϕ) . Thus, the motion equation of the multi-body dynamics model of the transmission line can be expressed as Eq. (1), which has 124 equations.

$$[m]\{\ddot{q}\} = Q \quad (1)$$

In Eq. (1), Q is the external force term, which can be expressed as the sum of gravity, the damping force, the spring force, and tension. The damping force inside the transmission line was

modeled using free vibration experiments of transmission line and the Rayleigh damping coefficient to analyze the dynamic behavior of the transmission line. In the free vibration test of transmission line, changes in the location of the end of the transmission line where deformation occurred because of the self-weight in the cantilever state were analyzed according to the transmission line length, and the Rayleigh damping coefficient was calculated using the amplitude ratio obtained through the free vibration test. The length of the actual transmission line is very long. Thus, it is difficult to obtain the amplitude through experiments. To overcome this, an amplitude ratio was curve-fitted using power equations, which provided an estimate of the Rayleigh damping coefficient^[10].

Assuming that the heights at the supporting points of both ends in the transmission line are the same and that the deflection curve has a parabolic shape, the deflection curve of the transmission line can be calculated as presented in Eq. (2) through cable deflection analysis.

$$y(x) = \frac{mgl^2}{2T} \left\{ \left(\frac{x}{l} \right) - \left(\frac{x}{l} \right)^2 \right\} \quad (2)$$

where, $m(kg/m)$ refers to the mass per unit length of transmission line, $T(N)$ is the tension, $l(m)$ is the span of transmission line and $g(m/s^2)$ is the gravity acceleration. Using 11.48m, which was the design sag in a general region where the snowing period was less than one month, a deflection curve of the transmission line was obtained first. Then, the previously modeled damping and spring forces were applied to the transmission line model to carry out the static deflection analysis. The analysis results exhibited that the error rate was less than 1%, which verified the accuracy when comparing the theoretical deflection curve and lumped mass location of the transmission line model.

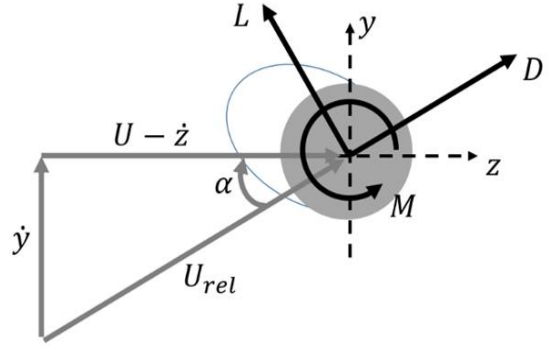


Fig. 3 Aerodynamic forces acting on transmission line

2.2 Wind load modeling of transmission line

Figure 3 shows the aerodynamic forces acting on transmission line. Once the wind load is applied to the ice accretion transmission line, a relative speed is applied because of the vertical speed of the transmission line and the wind speed. In Fig. 3, U (m/s) represents the wind speed; \dot{y} and \dot{z} mean vertical and lateral speeds of the transmission line, respectively; and U_{re} is the relative wind speed. The angle of attack α is expressed in Eq. (3). The force D , which was resistant against the wind load applied to the transmission line, is the drag force, and the force L , generated in the vertical direction of the load direction applied to the transmission line, is the lift force. These forces can be expressed by Eqs. (4) and (5), respectively.

$$\alpha = \tan^{-1} \left(\frac{\dot{y}}{U - \dot{z}} \right) \quad (3)$$

$$D = \frac{1}{2} \rho U_{re}^2 AC_D(\alpha) \quad (4)$$

$$L = \frac{1}{2} \rho U_{re}^2 AC_L(\alpha) \quad (5)$$

In Eqs. (4) and (5), $\rho(kg/m^3)$ is air density, A (mm^2) is area of receiving wind and C_L, C_D is lift and drag coefficient, respectively. Considering the angle of attack, the forces in the vertical and lateral directions are expressed in Eqs. (6) and (7), respectively.

$$F_y = L \cos(\alpha) + D \sin(\alpha) \quad (6)$$

$$F_z = -L \sin(\alpha) + D \cos(\alpha) \quad (7)$$

An oval shape was selected as the cross section of ice accretion: the shape has a high likelihood of galloping, and it occurs in a natural state that allows for simple modeling of the aerodynamic force. The ice accretion thicknesses in the normal, heavy, and most heavy snowfall regions were classified according to snow period and altitude above sea level^[11].

The angle of attack (α) of the oval ice accretion cross section was increased from 0° to 180° in 10° increments to carry out fluid analysis. The ice accretion thickness presented in Table 1 was considered, and the analysis region was set to be sufficiently large to prevent the effects of the side and the wake during fluid analysis. Figures 4 and 5 show the lift and drag coefficients of the oval ice accretion cross sections, respectively. The conductor directly exposed to the wind load was called No. 1, and the conductor that was hidden behind the No. 1 conductor that had a smaller wind load effect was called No. 2. Since the lift force occurred because of the asymmetry of the cross section as a result of the change in the angle of attack, the lift coefficient became a value that was close to zero because of

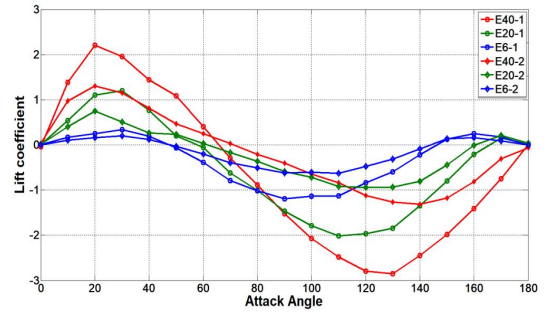


Fig. 4 Lift coefficient

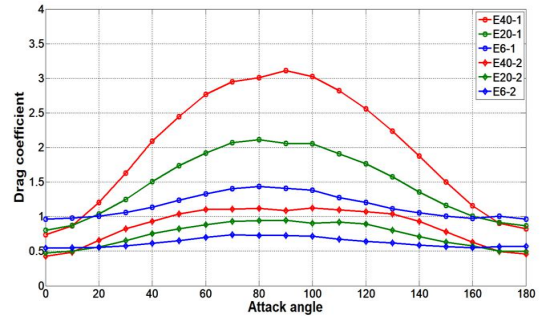


Fig. 5 Drag coefficient

the symmetry of the cross section when the angles of attack were 0° and 180° . When the angle of attack was between 90° to 180° , the lift force was applied in the opposite direction. Thus, the lift coefficient had a negative value. Since the drag force was proportional to the windward surface, it was increased as the ice accretion thickness increased, and the angle of attack was closer to 90° .

If the transmission line move only in the vertical direction and has a quasi steady state, the galloping occurs when the equivalent damping according to the angle of attack is changed to a negative value. This is called the Den Hartog Criterion, which is the necessary condition of galloping generation^[12].

The angle of attack at which galloping could occur was investigated by applying the aerodynamic coefficient obtained through the flow analysis to the Den Hartog Criterion, and galloping simulations of

Table 1 Icing thickness according to region

	Normal	Heavy snowfall	Most heavy snowfall
Icing thickness(mm)	6	20	40

both Nos. 1 and 2 conductors were performed with regard to the angle of attack that caused instability in the transmission line.

3. Galloping simulations

The behavior of the transmission line was analyzed after the wind speed was applied constantly at $10(m/s)$, starting at 80 sec when the static equilibrium was maintained, and was removed at 100 sec.

3.1 Results according to the spacer stiffness

The safety is increased with materials of higher spring stiffness, but the economic feasibility is decreased. Thus, it is important to select a spring stiffness value that is well balanced between safety and economic feasibility through galloping simulations according to the spacer stiffness. The galloping simulations were carried out while increasing the stiffness on a log scale from $0.01 N/m$ to $100kN/m$ to display a distinctive difference, since a mean value of the phase-to-phase distances was compared during galloping through the simulation. Figure 6 shows the comparison results of whether the phase-to-phase distance of $0.4 m$ was maintained, according to the spring stiffness. Once the spring stiffness exceeded $100N/m$, the spring was not significantly deformed, regardless of the spacer installation interval, but the approximate value of $0.4 m$ of phase-to-phase distance was maintained. The stiffness of the actual spring spacer material was approximately $130N/m$.

3.2 Results according to the spacer interval

The number of spacer damper installations and their intervals according to the steel tower span are specified in the construction standards for steel towers, which require a consistent interval of approximately $50 m$. When galloping occurs constantly,

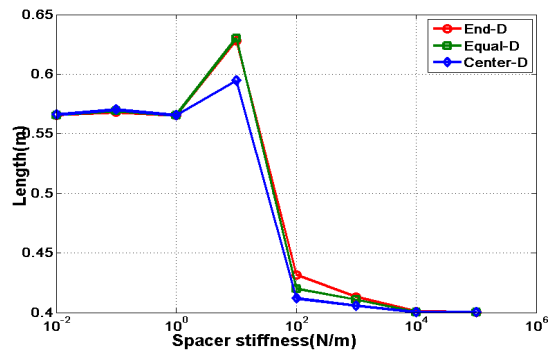


Fig. 6 Spacer length during galloping

it can lead to fatigue failure in the support points. If a spacer is installed intensively in the support point, fatigue failures can be prevented. This study carry out galloping simulations according to the stiffness and installation interval by modeling a total of nine phase spacers at a $500 m$ span. In the simulations, these cases were considered with regard to the interval of the spacer: nine spacers installed at every $50 m$ distance, nine spacers installed at the center intensively, and nine spacers installed at the support point intensively. The interval was set to have bilateral symmetry to follow the geometric sequence whose common ratio was two. The best performance was revealed when spacers were installed at the support point intensively, in which the reaction force of the support point, the amplitude in the vertical direction, and the acceleration were reduced by 5%, 10%, and 20% approximately.

4. Conclusions

This study modeled the transmission line with a number of lumped masses, springs, and dampers, and free vibration tests on the transmission line were conducted. The Rayleigh damping coefficient was also estimated using the amplitude ratio and the natural frequency, and the obtained results were

applied to the transmission line modeling. The galloping generation conditions were identified through the flow analysis, and the wind load was modeled to perform galloping simulations.

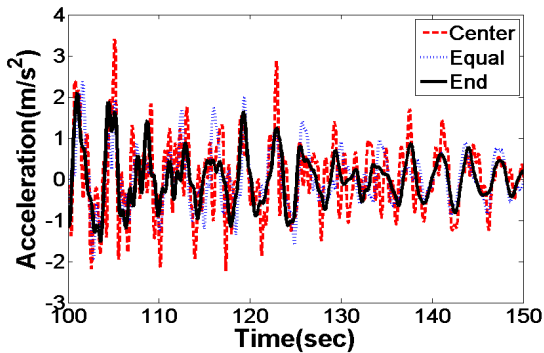


Fig. 7 Acceleration of center node

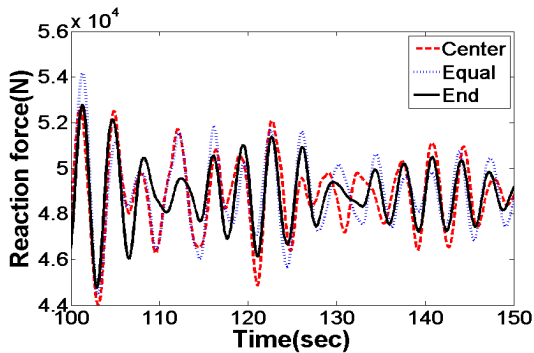


Fig. 8 Reaction force of the support

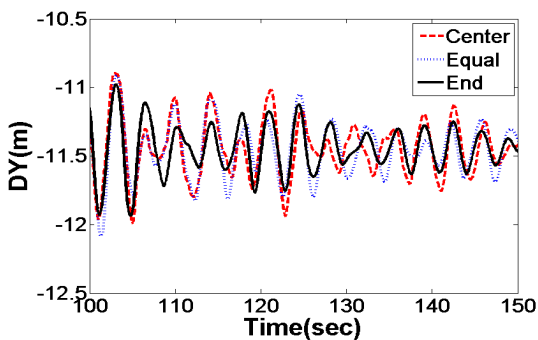


Fig. 9 Displacement of center node

The analysis of the effect of spring stiffness and spacing on galloping was carried out after modeling the spring spacer between phases of bundled transmission line, and the stiffness value of the spring spacer currently installed was found to be suitable. The reaction force at the support point and the acceleration were reduced by more than 5% and 20%, respectively, to achieve better results when the spacers were installed at both supporting points intensively than those of the currently installed spacer interval.

REFERENCES

1. Koo, J. R. and Bae, Y. C., "Protection method of ice and snow failure at the power transmission line", Proc. of the Korean Society for Noise and Vibration Engineering, Vol.2015, No.4, pp.735-738, 2015.
2. Wang, J. and Lilien, J. L., "A new theory for torsional stiffness of multi-span bundle overhead transmission lines", IEEE transactions on power delivery, Vol. 13, No. 4, pp.1405-1411, 1998.
3. Hu, J., Song, Z., Ma, J. and Wu, S., "Model for Comprehensive Simulation of Overhead High Voltage Power Transmission Line Galloping and Protection", Annual Report Conference on Electrical Insulation and Dielectric Phenomena, pp.190-193, 2006.
4. Cho, J. U. and Han, M. S., "Study on the Vibration Analysis of Damper Clutch Spring", Journal of the Korean Society of Manufacturing Process Engineers, Vol. 10, No. 4, pp22-30, 2011.
5. Kim, Y. J., Ro, S. H., Shin, H. B., Shin, Jung, K. S., and Nam, K. D., "Effects of Design Alterations on the Vibration Suppression of a Machine Tool Structure", Journal of the Korean Society of Manufacturing Process Engineers, Vol. 15, No. 3, pp122-129, 2016.
6. Davison, A. E., "Dancing conductors",

Transactions of the American Institute of Electrical Engineers, Vol. 49, No. 4, pp.1444-pp.1449, 1930

7. Den Hartog, J. P., "Transmission Line Vibration Due to Sleet", Transactions of the American Institute of Electrical Engineers, Vol. 51, No. 4, 1932.
8. Kim, J. W. and Sohn J. H., "Multibody dynamics study on galloping of power transmission line", Journal of Mechanical Science and Technology, Vol. 32, No. 8, pp.3597-3602, 2018.
9. Kwak, M. K., Shin, J. H. and Koo, J. R., "Dynamic Modeling of Bundled transmission line and Vibration Experiment", KSNVE fall conference, pp728-734, 2015.
10. Alipour, A. and Zareian, F., "Study Rayleigh damping in structures Unceratinities and treatments", proceedings of 14th Word conference on Earthquake Engineering, Beijing, China, 2008.
11. Lilien, J. L., "State of the art of conductor galloping", Technical Brochure CIGRE N° 322, Task Force B2.11.06, 2007.
12. Nikitas, N. and Macdonald, J. H. G., "Misconceptions and Generalizations of the Den Hartog Galloping Criterion", Journal of Engineering Mechanics, Vol. 140, No. 4, 2013.